

Fabrication of Iron-based Oxygen Carriers on Various Supports for Chemical Looping Hydrogen Generation

Hsuan-Chih Wu, Young Ku, Yi-Syuan Huang, Niels Michiel Moed*

Department of Chemical Engineering, National Taiwan University of Science and Technology, Taipei 106, Taiwan

ABSTRACT

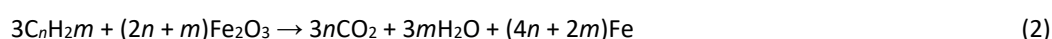
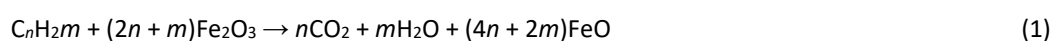
$\text{Fe}_2\text{O}_3/\text{Al}_2\text{O}_3$ and $\text{Fe}_2\text{O}_3/\text{TiO}_2/\text{Al}_2\text{O}_3$ oxygen carriers were fabricated and evaluated for chemical looping hydrogen generation (CLHG) using a TGA system and a fixed-bed reactor. Oxygen carriers were converted to around 33% in a fixed-bed reactor to ensure uniform reduction. The reduced oxygen carrier was tested for steam generation, where in all cases $\text{Fe}_2\text{O}_3/\text{Al}_2\text{O}_3$ displayed a better conversion than $\text{Fe}_2\text{O}_3/\text{TiO}_2/\text{Al}_2\text{O}_3$. It was found that increasing the reaction temperature from 800 to 850 °C had little effect for either oxygen carrier, but a further increase to 900 °C resulted in an increased steam conversion. A higher steam flow rate caused a lower overall steam conversion but a higher H_2 production. A higher feed rate of reduced oxygen carrier led to a higher steam conversion up to a rate of 18.4 and 14.9 g min^{-1} for $\text{Fe}_2\text{O}_3/\text{Al}_2\text{O}_3$ and $\text{Fe}_2\text{O}_3/\text{TiO}_2/\text{Al}_2\text{O}_3$, respectively. A final comparison was performed with up to 50 redox cycles, where $\text{Fe}_2\text{O}_3/\text{Al}_2\text{O}_3$ showed superior reactivity in the first cycles but ended at a conversion of 54.6% with $\text{Fe}_2\text{O}_3/\text{TiO}_2/\text{Al}_2\text{O}_3$ ending at a conversion of 64.6%.

Keywords: Chemical looping hydrogen generation (CLHG), $\text{Fe}_2\text{O}_3/\text{Al}_2\text{O}_3$, $\text{Fe}_2\text{O}_3/\text{TiO}_2/\text{Al}_2\text{O}_3$, Oxygen carrier, Moving-bed reactor

1 INTRODUCTION

Hydrogen is an environmentally friendly energy option which can address issues such as global climate change, air pollution and energy security. The ways to produce hydrogen are many, with the steam-iron process (SIP) being used since the early 20th century (Hurst, 1939). In this process, iron species are employed to split water molecules by binding to the oxygen atoms, generating iron oxide and hydrogen. This process can be implemented in continuous reduction and oxidation cycles of the iron oxide. However, the reactivity of iron oxides is significantly reduced after repeated redox cycling, resulting in poor hydrogen generation (Kierzkowska *et al.*, 2010). Iron oxides are also frequently employed as oxygen carrier in the chemical looping process (CLP) for efficient fuel combustion with generation of high concentration CO_2 . The integration of the steam-iron process with chemical looping, termed as chemical looping hydrogen generation (CLHG), generates high-purity CO_2 and H_2 simultaneously by using an Fe-based oxygen carrier operating in a moving-bed reactor (Tong *et al.*, 2013).

Chemical looping hydrogen generation employs a fuel reactor for combustion of fuel and generation of CO_2 , a steam reactor for generation of H_2 and an air reactor for further oxidation of the oxygen carrier. Fuels react with the oxygen carriers in the fuel reactor, with the product being a gas that is mainly composed of CO_2 and H_2O . The reactions are expressed by the following Eqs. (1)–(2).



OPEN ACCESS

Received: June 19, 2020

Revised: October 13, 2020

Accepted: October 23, 2020

* Corresponding Author:

nikolai.moed@gmail.com

Publisher:

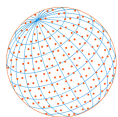
Taiwan Association for Aerosol
Research

ISSN: 1680-8584 print

ISSN: 2071-1409 online

 Copyright: The Author(s).

This is an open access article distributed under the terms of the [Creative Commons Attribution License \(CC BY 4.0\)](https://creativecommons.org/licenses/by/4.0/), which permits unrestricted use, distribution, and reproduction in any medium, provided the original author and source are cited.



CO₂ can be purified from the gas stream through condensation of the water vapor. The reduced oxygen carriers are then oxidized by steam to generate hydrogen as demonstrated by Eqs. (3)–(4).



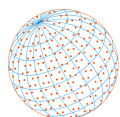
The partly oxidized Fe-based oxygen carriers are subsequently regenerated by further oxidation in the air reactor as illustrated by Eq. (5).



Sintering and attrition during continuous and high temperature operations would decrease the effectiveness of these iron-based oxygen carriers. The reactivity and recyclability of iron-based oxygen carriers was reported to be considerably enhanced by coupling mixed metal oxides to prevent the sintering of oxygen carriers and to enhance their mechanical strength. A wide range of metal oxides can be utilized as support materials, such as Al₂O₃, TiO₂, ZrO₂, SiO₂ and bentonite, each with their own advantages and disadvantages. Fe₂O₃ is commonly used with Al₂O₃ as a support material, where Al₂O₃ not only enhances the mechanical strength of Fe₂O₃ but also increases the reactivity. Cho *et al.* (2006), for example, mixed 60 wt% Fe₂O₃ with 40 wt% Al₂O₃ to fabricate the oxygen carriers by the freeze-granulation technique. Experimental results illustrated that the fabricated oxygen carriers delivered a high reduction and oxidation reactivity without noticeable carbon formation, as methane was used as fuel. Abad *et al.* (2007) utilized Fe₂O₃/Al₂O₃ oxygen carriers, fabricated with the same weight ratio by freeze granulation technique, in a continuous unit at temperatures from 800 to 950°C. Experiments using natural gas or syngas were carried out for a total of 40 hours, without evident signs of deactivation, agglomeration, carbon deposition and with very low attrition for the fabricated oxygen carriers. Chiu *et al.* (2014) observed that FeAl₂O₄ is formed during CLP with Fe₂O₃ and Al₂O₃. This is still an effective oxygen carrier and possesses a higher melting point than FeO, mitigating agglomeration of pellets.

TiO₂ is another commonly used support metal oxide. Mattisson *et al.* (2004) fabricated various Fe₂O₃/Al₂O₃/TiO₂ oxygen carriers, and the XRD patterns revealed that major reactions occurred between Fe₂O₃ and TiO₂. The amounts of Fe₂O₃ and TiO₂ affected the crush strength of the fabricated oxygen carriers, with oxygen carriers containing 60% Fe₂O₃ outperforming those containing 40%. Ilmenite, a titanium-iron-oxide mineral with the formula FeTiO₃, was reported by Cuadrat *et al.* (2011) to be a reliable and effective oxygen carrier for the chemical looping combustion of coal and petroleum coke as solid fuels for energy production. Not only did this achieve high CO₂ capture efficiencies, no noticeable decrease in the conversion of ilmenite was observed. Adániz *et al.* (2010) indicated that the reactivity of ilmenite stabilized after several redox operation cycles in a TGA system, which is possibly attributed to the increased porosity and the structural changes during the chemical looping operation. However, Zhao and Shadman (1990) noted that phase segregation of iron oxide and titanium oxide took place over multiple redox cycles. Iron oxide was observed to migrate out to the surface from the FeTiO₃ during the oxidation, as shown by XRD analyses. This could fracture the ilmenite particles and lower the particle strength. Fe₂O₃/Al₂O₃ and Fe₂O₃/TiO₂/Al₂O₃ oxygen carriers were fabricated and assessed by Lo (2014) for their applications in chemical looping combustion and chemical looping hydrogen generation. Both oxygen carriers demonstrated high effectivity and recyclability with an iron, titanium and aluminum ratio of 7:1:2 exhibiting excellent reduction over multiple cycles, possibly due to its high oxygen carrying capacity.

The objective of this paper is to investigate the feasibility and effectivity of the addition of TiO₂ to Fe₂O₃/Al₂O₃ oxygen carriers for use in a CLHG system. To accomplish this comparison, oxygen carriers were fabricated and uniformly reduced in a fixed-bed reactor system. The reduced oxygen carriers were subsequently partially regenerated in a moving-bed reactor system using steam oxidation. Both freshly fabricated and regenerated oxygen carriers were tested in a TGA system over 50 cycles to test recyclability and long-term regeneration efficiency.



2 METHODS

2.1 Preparation and TGA Reactivity Testing of Iron-based Oxygen Carriers

$\text{Fe}_2\text{O}_3/\text{Al}_2\text{O}_3$ and $\text{Fe}_2\text{O}_3/\text{TiO}_2/\text{Al}_2\text{O}_3$ were fabricated to serve as oxygen carriers in this study. Hematite, alumina and titania particles were mixed thoroughly in deionized water at room temperature. The $\text{Fe}_2\text{O}_3/\text{Al}_2\text{O}_3$ oxygen carriers were formulated with 60% hematite (99.9% Fe_2O_3 , China Steel) and 40% alumina (99% Al_2O_3 , Chin Jung) while the $\text{Fe}_2\text{O}_3/\text{TiO}_2/\text{Al}_2\text{O}_3$ was formulated with 70% hematite, 20% alumina and 10% titania (99% TiO_2 , Unique Enterprise Co.). The well-mixed slurry was desiccated at 130°C for 12 hours and subsequently pulverized and screened for particles to a size between 1.2 and 1.4 mm. The particles were afterward sintered for 2 hours in a muffle furnace at 1200°C for $\text{Fe}_2\text{O}_3/\text{TiO}_2/\text{Al}_2\text{O}_3$ and at 1300°C for $\text{Fe}_2\text{O}_3/\text{Al}_2\text{O}_3$, which were the optimum sintering temperatures according to Lo (2014). The surface of the fabricated oxygen carriers was subsequently characterized using a D2 PhASER X-Ray Diffractor by Bruker and a JSM-6500F Field Emission Scanning Electron Microscope (FE-SEM) by JOEL.

The reactivity of fabricated oxygen carriers was analyzed by a Netzsch STA 449F3 thermogravimetric analyzer (TGA). A portion of 200 mg oxygen carriers was loaded in an alumina crucible of the TGA, the temperature of the TGA chamber was elevated with a ramping rate of $30^\circ\text{C min}^{-1}$ in air atmosphere and eventually kept at 900°C . Residual air in the TGA chamber was purged by nitrogen for 5 minutes before 200 mL min^{-1} syngas (composed of 10% CO, 10% H_2 and 80% N_2) was introduced into the TGA chamber for reducing the fabricated oxygen carriers. After the oxygen carriers were reduced, 200 mL min^{-1} air was then introduced to oxidize the reduced oxygen carriers. The reduction and oxidation procedure was replicated for up to 50 cycles to determine the recyclability of fabricated iron-based oxygen carriers.

2.2 Reduction Tests Using the Fixed-bed Reactor System

Reduction in the Fixed-Bed Reactor System was tested, with the goal of reducing oxygen carriers by 33% for further use in following tests. The fixed-bed reactor system consisted of a stainless-steel tubular reactor with a PID-controlled heating element. A plate with sixteen 0.25 mm apertures was located in the lower part of the reactor for supporting fabricated iron-based oxygen carriers. Oxygen carriers were added to the system, where the mass added was adjusted for particle density. The temperature of the loaded reactor was then raised and eventually kept at the chosen operating temperature, which was originally 650°C but was raised to 800°C for $\text{Fe}_2\text{O}_3/\text{Al}_2\text{O}_3$, as this oxygen carrier could not be sufficiently reduced at 650°C . A hydrogen/nitrogen gas mixture was subsequently introduced into the fixed-bed reactor to reduce fabricated oxygen carriers. The outlet gas stream from the fixed-bed reactor was passed through a cold trap to condense water vapor, and was then analyzed by a gas chromatograph equipped with a thermal conductivity detector (GC-TCD, China Chromatography 2000) to determine the concentrations of hydrogen and nitrogen. The remaining reduced $\text{Fe}_2\text{O}_3/\text{Al}_2\text{O}_3$ and $\text{Fe}_2\text{O}_3/\text{Al}_2\text{O}_3/\text{TiO}_2$ oxygen carriers were collected for further experiments carried out in the moving-bed reactor system.

2.3 Reaction Tests in the Moving-Bed Reactor System

A schematic diagram of the moving-bed reactor employed in this study is shown in Fig. 1. The reactor was composed of a stainless-steel tube covered with a PID-controlled electric heating element. The temperature inside the 60 cm reactor tube was measured at 3 points, located at 10, 30 and 50 cm from either the gas inlet or gas outlet. Roughly 2.5 kg reduced $\text{Fe}_2\text{O}_3/\text{Al}_2\text{O}_3$ and 2.1 kg reduced $\text{Fe}_2\text{O}_3/\text{Al}_2\text{O}_3/\text{TiO}_2$ oxygen carriers collected from the fixed-bed reactor system were packed in the reactor before operation. In addition, reduced oxygen carriers were continuously fed into the packed moving-bed reactor by a screw conveyer after the reactor was heated up to predetermined temperatures. Steam and nitrogen were correspondingly introduced into the reactor for oxidizing the reduced oxygen carriers to generate hydrogen. The partially oxidized oxygen carriers were collectively removed out of the reactor by another screw conveyor. The outlet gas stream from the moving-bed reactor was cooled by a cold trap to condense water vapor and analyzed by a GC-TCD (China Chromatography 2000) to detect the concentration of hydrogen.

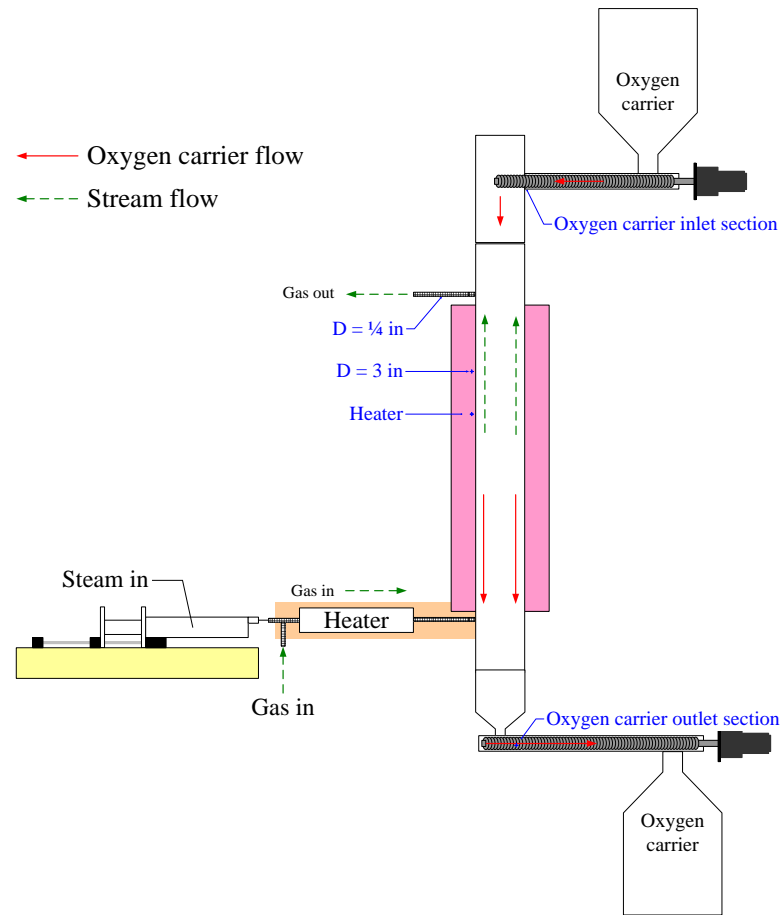
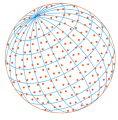


Fig. 1. Schematic diagram of the moving-bed reactor system used in this study.

3 RESULTS AND DISCUSSION

3.1 Conversions of Fabricated Iron-based Oxygen Carriers

The reactivity of fabricated $\text{Fe}_2\text{O}_3/\text{Al}_2\text{O}_3$ and $\text{Fe}_2\text{O}_3/\text{TiO}_2/\text{Al}_2\text{O}_3$ oxygen carriers were examined in a TGA using syngas as reducing gas for 50 successive redox cycles. As depicted in Fig. 2, the reduction of $\text{Fe}_2\text{O}_3/\text{Al}_2\text{O}_3$ was about 68% initially and gradually decreased to 51% after 50 cycles. The reduction of $\text{Fe}_2\text{O}_3/\text{TiO}_2/\text{Al}_2\text{O}_3$ increased slightly in the first 3 cycles and further after about 30 cycles after which it was maintained at around 60% up to the end of the 50-cycle operation. This indicates that the fabricated iron-based oxygen carriers are capable of providing reasonable recyclability for continuous redox operation of syngas chemical looping combustion.

Based on the oxygen balance, the conversion of fabricated oxygen carriers (X_{OC}) is defined as:

$$X_{OC} = \frac{\int (F_{\text{H}_2, \text{in}} - F_{\text{H}_2, \text{out}}) dt}{3N_{\text{Fe}_2\text{O}_3}} \quad (6)$$

where the Fe fraction of oxygen carriers is reduced as follows:



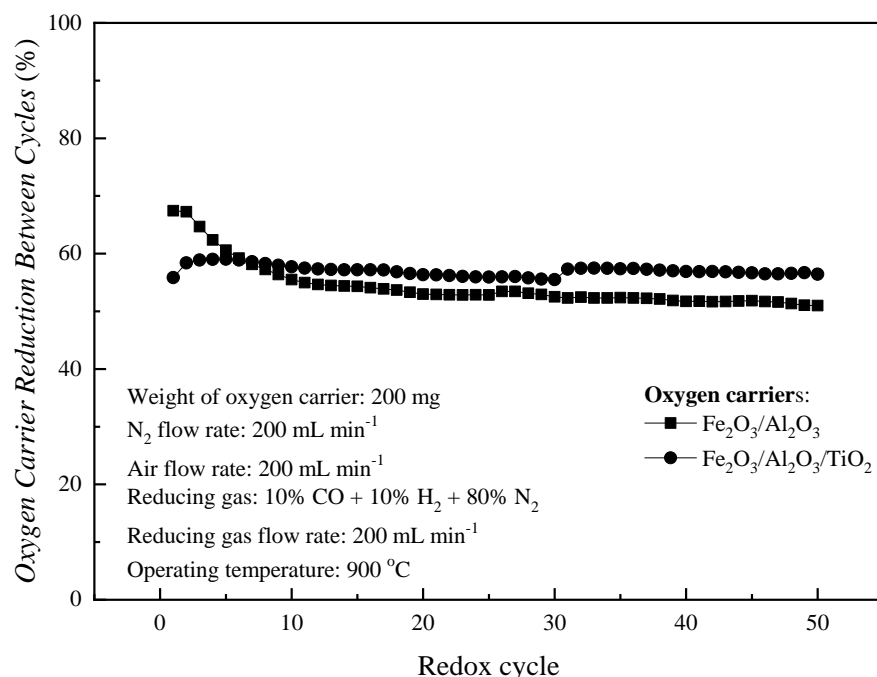
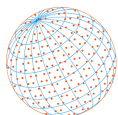


Fig. 2. Conversion of fabricated iron-based oxygen carriers employed in a TGA for 50 redox cycles at 900°C.

Fig. 3 displays the reduction of fabricated Fe₂O₃/TiO₂ and Fe₂O₃/TiO₂/Al₂O₃ oxygen carriers in the fixed-bed reactor, with Fe₂O₃/TiO₂/Al₂O₃ oxygen carriers reaching about 33% reduction after the introduction of the hydrogen/nitrogen gas mixture for 140 minutes at a temperature of 650°C, corresponding to the oxygen utilization by hydrogen via the reduction of Fe₂O₃ to form FeO (Fan, 2010). However, the reduction of fabricated Fe₂O₃/Al₂O₃ conducted at 650°C was observed to reach only about 23% conversion after a 90-minute operation, much lower than that for Fe₂O₃/TiO₂/Al₂O₃. Higher conversion (approximately 33%) was achieved for the reduction of fabricated Fe₂O₃/Al₂O₃ oxygen carriers operated at 800°C for operation time greater than 150 minutes. The higher reduction from TiO₂ addition has been discussed by Li *et al.* (2011), who stated that while the addition of TiO₂ does not seem to significantly reduce the activation energy for reduction, it does significantly lower the energy barrier for O²⁻ migration within the dense solid phase, enhancing the O²⁻ diffusivity.

3.2 Hydrogen Generation in the Moving-Bed System with Reduced Fe₂O₃/Al₂O₃ Oxygen Carriers

For experiments regarding to the chemical looping hydrogen generation by the reaction between steam and reduced iron-based oxygen carriers, the hydrogen yield (X_s) is calculated as:

$$X_s = \frac{F_{H_2,out}}{F_{H_2O,in}} \quad (10)$$

where $F_{H_2O,in}$ is the input molar flow rate (mmole min⁻¹) of steam; $F_{H_2,out}$ is the output molar flow rate (mmole min⁻¹) of hydrogen. CLHG experiments were performed with Fe₂O₃/Al₂O₃ oxygen carriers at a temperature range of 800–900°C. As shown in Fig. 4, steam conversion was similar at 800 and 850°C but slightly increased for experiments conducted at 900°C. Sun *et al.* (2015) examined the hydrogen conversion in a CLHG system with various oxygen carriers consisting of Fe₂O₃, CeO₂ and Al₂O₃. They stated that hydrogen yield was doubled and even tripled when increasing the Fe₂O₃ content of oxygen carriers from 45% to 55% and 65%, respectively, at an operating temperature of 900°C. The effect of operating temperature on hydrogen production was found to be insignificant within the range of 850 to 950°C, with hydrogen yield and steam

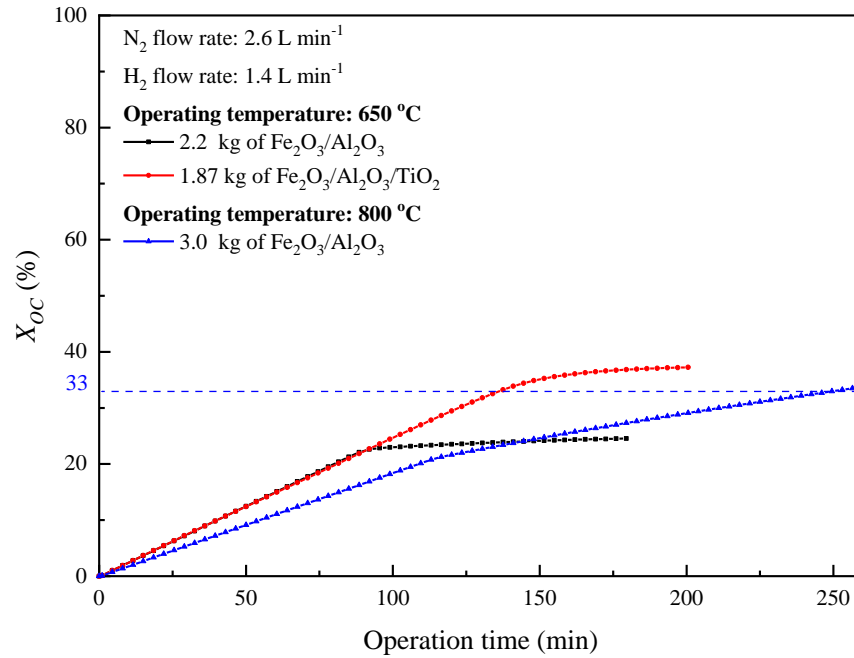
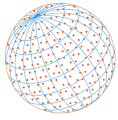


Fig. 3. Conversions of various fabricated iron-based oxygen carriers reduced by hydrogen in the fixed-bed reactor at 650°C and 800°C.

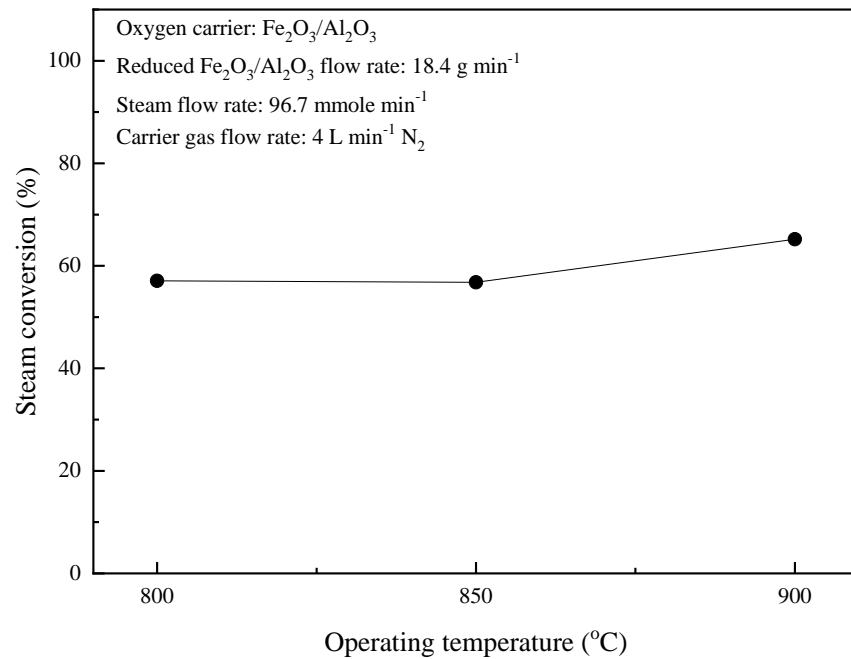


Fig. 4. Effect of operation temperature on the hydrogen flow rate, hydrogen concentration and steam conversion for CLHG with reduced Fe₂O₃/Al₂O₃ operated in the moving-bed reactor.

conversion increasing with temperature up until 900°C but decreased at 950°C. This increase is comparable to the results observed in this study. The steam conversion by the reduced Fe₂O₃/Al₂O₃ oxygen carriers was noticed to be slightly enhanced with operating temperature, which was calculated to be about 65% for experiments conducted at 900°C.

Chemical looping hydrogen generation by reduced Fe₂O₃/Al₂O₃ oxygen carriers with steam at 900°C were performed at various steam flow rates. As illustrated in Fig. 5, both hydrogen concentration and flow rate were evidently enhanced for experiments conducted at higher steam

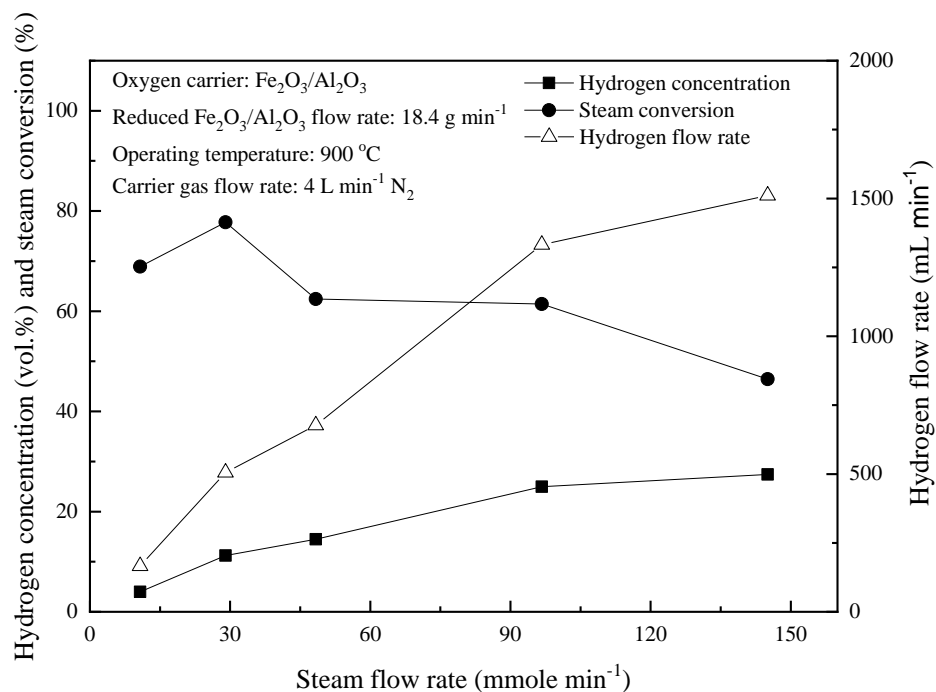
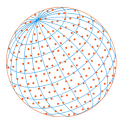


Fig. 5. Effect of steam flow rate on the hydrogen flow rate, hydrogen concentration and steam conversion for CLHG with reduced Fe₂O₃/Al₂O₃ operated in the moving-bed reactor.

flow rates, whereas the calculated steam conversions were decreased. The hydrogen flow rate of around 1.4 L min⁻¹ was achieved with a steam flow rate of 96.7 mmole min⁻¹, which led to a steam conversion of around 60%. Lo (2014) also stated that experiments using Fe₂O₃/TiO₂ oxygen carriers operated at higher steam flow rates might exhibit accelerated oxidation of FeO and Fe to Fe₃O₄, while hydrogen generation and steam conversion was reduced for experiments. Yang *et al.* (2008) demonstrated that the conversion of steam by iron is limited by the oxidation state of the iron and the steam flow rate in the steam reactor, where operations with more steam enhances the oxidation of iron and the production of hydrogen. Therefore, from an operating perspective, if hydrogen yield is the target, a higher steam flow rate is optimal within the described range. The same is true for hydrogen concentration. The lowered steam conversion efficiency, however, will lead to an increase in operating cost. This will lead to a consideration having to be made between operating cost and yield, which will depend on the specific operating system.

As shown in Fig. 6, both hydrogen concentration and flow rate were significantly increased for experiments conducted at a reduced Fe₂O₃/Al₂O₃ feeding rate lower than 18.4 g min⁻¹. However, hydrogen concentration remained at about 26% for experiments conducted at a feeding rate of reduced Fe₂O₃/Al₂O₃ higher than 18.4 g min⁻¹. Approximately 65% of steam conversion was achieved for experiments conducted with a feeding rate of reduced Fe₂O₃/Al₂O₃ higher than 18.4 g min⁻¹. A similar observation was reported by previous researchers, (Yang *et al.*, 2008) where steam conversion was increased for experiments conducted at higher feeding rate of reduced oxygen, until a certain steam conversion was reached.

XRD analysis for the fresh, reduced and partially oxidized Fe₂O₃/Al₂O₃ oxygen carriers are demonstrated in Fig. 7. The fresh oxygen carrier was determined to be completely comprised of Fe₂O₃ and Al₂O₃. The partial oxidation was conducted through steam reduction in the moving bed reactor at 900 °C at an oxygen carrier flow rate of 18.4 g min⁻¹ and a steam flow rate of 96.7 mmole min⁻¹. Fe₂O₃ was transformed to FeO, Fe₃O₄, and Fe after reduction while Al₂O₃ remained largely present, with some FeAl₂O₄ being formed. This observation was somewhat different from the results described by Cabello *et al.* (2014), noting that FeAl₂O₄ was the only stable Fe-based phase after reduction. After partial oxidation in the steam reactor, the previously formed Fe and FeO were observed to be oxidized primarily to Fe₃O₄.

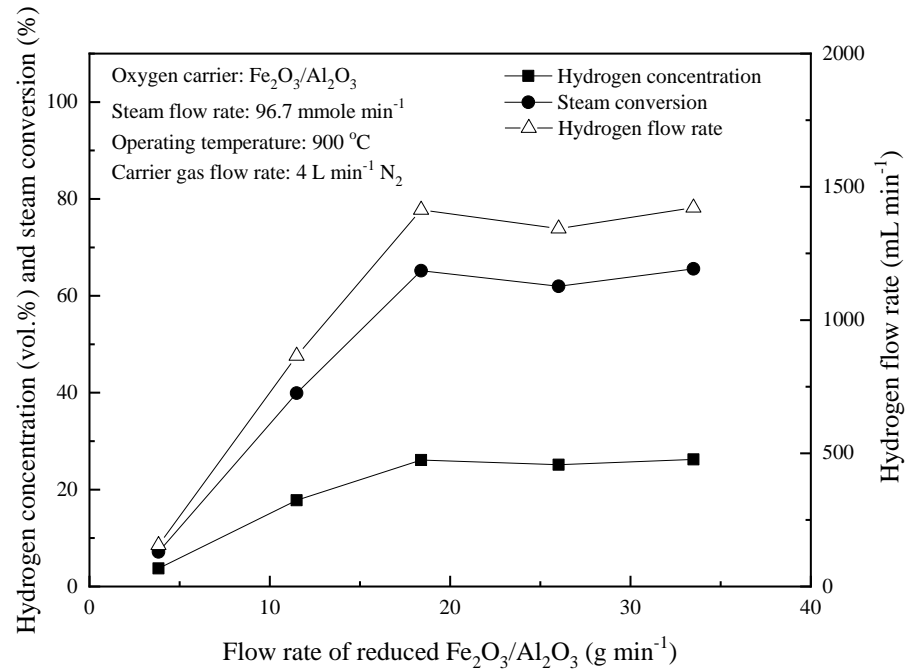
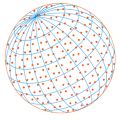


Fig. 6. Effect of oxygen carrier feeding rate on the hydrogen flow rate, hydrogen concentration and steam conversion for CLHG with reduced $\text{Fe}_2\text{O}_3/\text{Al}_2\text{O}_3$ operated in the moving-bed reactor.

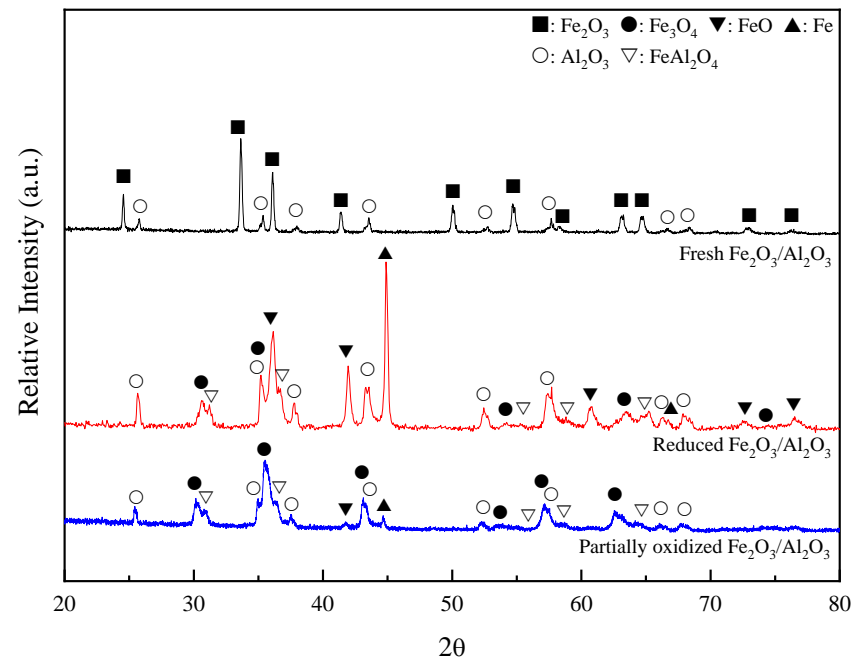


Fig. 7. X-ray diffraction patterns of fresh, reduced and partially oxidized $\text{Fe}_2\text{O}_3/\text{Al}_2\text{O}_3$ oxygen carriers employed for CLHG.

3.3 Hydrogen Generation in the Moving-bed System with Reduced $\text{Fe}_2\text{O}_3/\text{TiO}_2/\text{Al}_2\text{O}_3$ Oxygen Carriers

Chemical looping hydrogen generation by reduced $\text{Fe}_2\text{O}_3/\text{TiO}_2/\text{Al}_2\text{O}_3$ with steam was conducted in the moving-bed reactor operated at 800, 850 and 900°C. As illustrated in Fig. 8, steam conversion slightly decreased with temperature at a steam flow rate at 29 mmole min^{-1} , in particular when increasing the temperature from 800 to 850°C. These results are not consistent with those

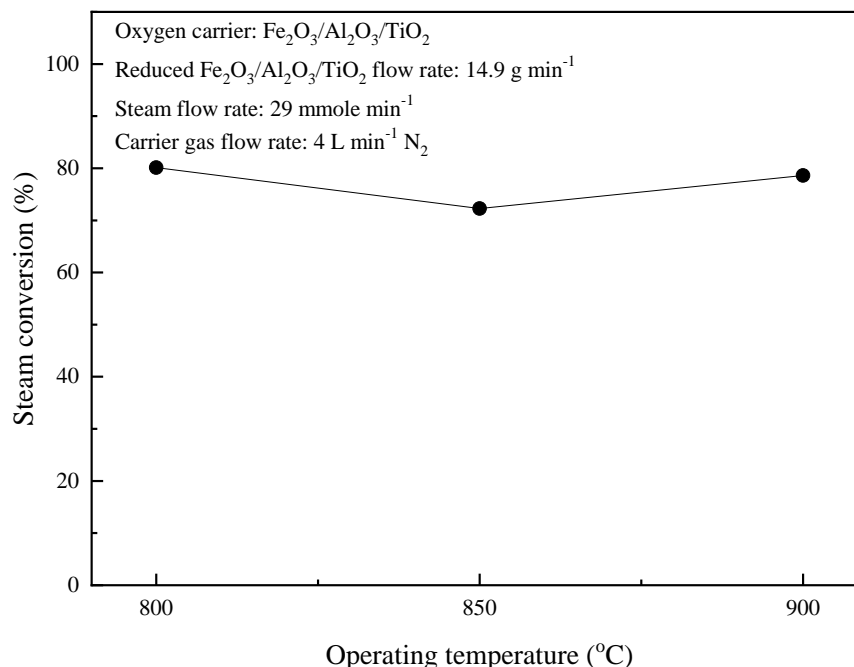
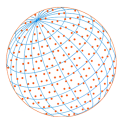


Fig. 8. Effect of operation temperature on the hydrogen flow rate, hydrogen concentration and steam conversion for CLHG with reduced $\text{Fe}_2\text{O}_3/\text{Al}_2\text{O}_3/\text{TiO}_2$.

observed in Fig. 4 using $\text{Fe}_2\text{O}_3/\text{Al}_2\text{O}_3$ and those reported by Sun *et al.* (2015), which both exhibited an increase in hydrogen yield for reactions operated at elevated temperatures. Sun *et al.* (2015), however, did find a decrease in hydrogen yield and steam conversion when increasing their reaction temperature from 900–950°C. The temperature at which this takes place likely depends on the materials used to fabricate oxygen carriers, in this case the TiO_2 not being used by Sun *et al.* (2015) and in experiments shown in Fig. 4.

As demonstrated in Fig. 9, the hydrogen concentration and flow rate of the outlet gas stream increased with the steam flow rate, whereas steam conversion was decreased for experiments conducted with $\text{Fe}_2\text{O}_3/\text{TiO}_2/\text{Al}_2\text{O}_3$. The concentration of hydrogen in the outlet gas stream was increased from about 12 to 22% when the steam flow rate was increased from 29 to 97 mmole min^{-1} . A hydrogen flow rate of nearly 1.2 L min^{-1} was maintained for experiments conducted with a steam flow rate greater than 97 mmole min^{-1} . This corresponds with the results reported by Lo (2014), which showed that steam conversion was reduced for experiments conducted at higher steam flow rates by $\text{Fe}_2\text{O}_3/\text{TiO}_2$ oxygen carriers. From an operating perspective, a higher steam flow rate increases hydrogen concentration and flow rate, leading to higher yields, within the tested range. But as mentioned in Fig. 5, the increased steam flow rate increased operating costs so that optimization will have to be done for the individual system to determine the optimal tradeoff between cost and yield.

As demonstrated in Fig. 10, the hydrogen concentrations of the outlet gas stream were found to be increased with greater oxygen carrier flow rate for experiments carried out with reduced $\text{Fe}_2\text{O}_3/\text{TiO}_2/\text{Al}_2\text{O}_3$ flow rate up to 14.9 g min^{-1} . At higher flow rates steam conversion was maintained at around 78% with a hydrogen flow rate of about 0.5 L min^{-1} . The effect of oxygen carrier flow rate for experiments conducted with reduced $\text{Fe}_2\text{O}_3/\text{TiO}_2/\text{Al}_2\text{O}_3$ are comparable to those conducted with reduced $\text{Fe}_2\text{O}_3/\text{Al}_2\text{O}_3$, as illustrated in Fig. 6.

XRD analysis was performed for the fresh, reduced and partially oxidized $\text{Fe}_2\text{O}_3/\text{TiO}_2/\text{Al}_2\text{O}_3$ oxygen carriers, as shown in Fig. 11. Comparing the XRD patterns shown in Fig. 7 for $\text{Fe}_2\text{O}_3/\text{Al}_2\text{O}_3$, Fe_2O_3 was reduced to Fe_3O_4 , and Fe, with no FeO being detected. Zieliński *et al.* (2010) found that in the three-step reduction of Fe_2O_3 with H_2 as a fuel gas, the final step of FeO to Fe can be so fast that FeO is not detected by XRD. They found that the rate of this reduction depends on the ratio of H_2 fuel gas to the H_2O formed in the reaction, with FeO being immediately reduced at low H_2O and high H_2 concentrations. After partial oxidation the Al species were completely

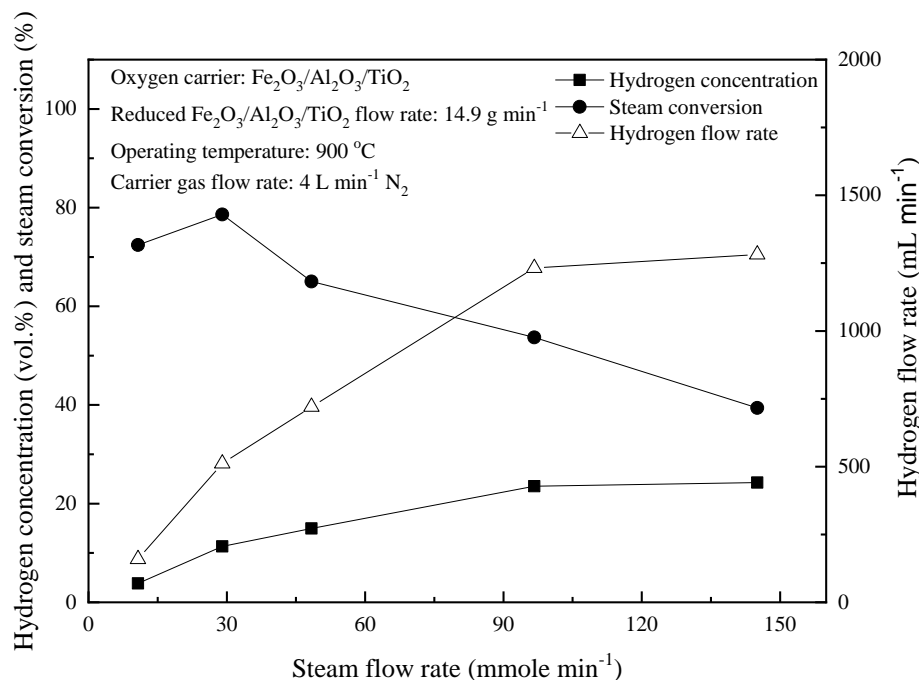
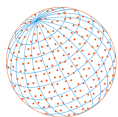


Fig. 9. Effect of steam flow rate on the hydrogen flow rate, hydrogen concentration and steam conversion for CLHG with reduced $\text{Fe}_2\text{O}_3/\text{Al}_2\text{O}_3/\text{TiO}_2$.

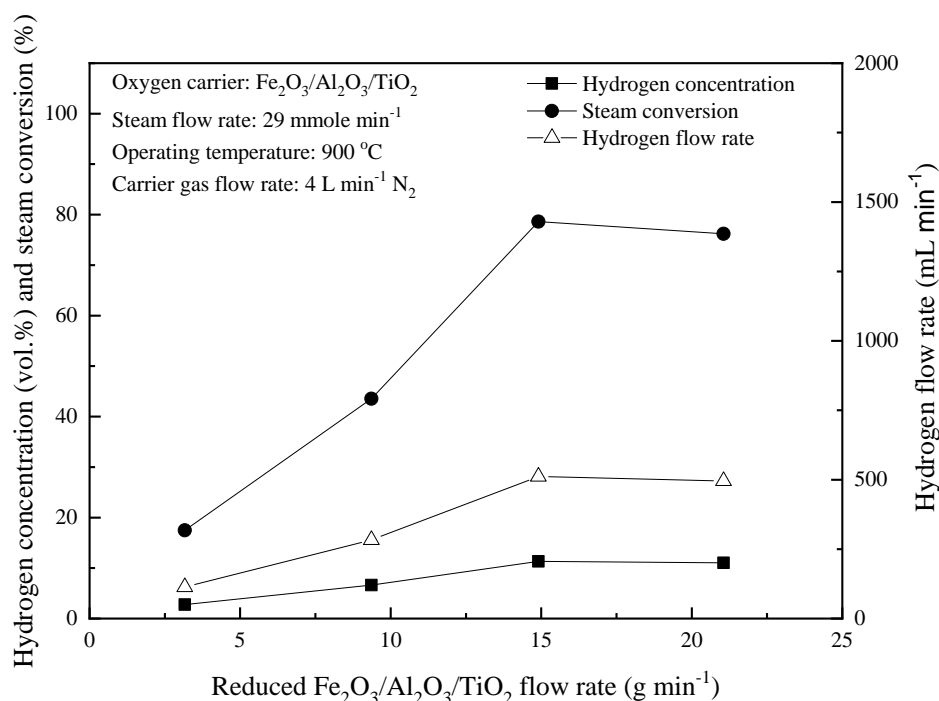


Fig. 10. Effect of oxygen carrier feeding rate on the hydrogen flow rate, hydrogen concentration and steam conversion for CLHG with reduced $\text{Fe}_2\text{O}_3/\text{Al}_2\text{O}_3/\text{TiO}_2$.

oxidized to FeAl_2O_4 , while in Fig. 7 it exists as both Al_2O_3 and FeAl_2O_4 . This is likely due to influence of the lower Al fraction in $\text{Fe}_2\text{O}_3/\text{TiO}_2/\text{Al}_2\text{O}_3$, as Al_2O_3 made up only 20% of the composition for $\text{Fe}_2\text{O}_3/\text{TiO}_2/\text{Al}_2\text{O}_3$, instead of 40% for $\text{Fe}_2\text{O}_3/\text{Al}_2\text{O}_3$. Titanium was present as Fe_2TiO_5 in the fresh $\text{Fe}_2\text{O}_3/\text{TiO}_2/\text{Al}_2\text{O}_3$ and was transformed to Fe_2TiO_4 after reduction. However, titanium species were not observed in the XRD pattern for the partially oxidized oxygen carrier, with the previously

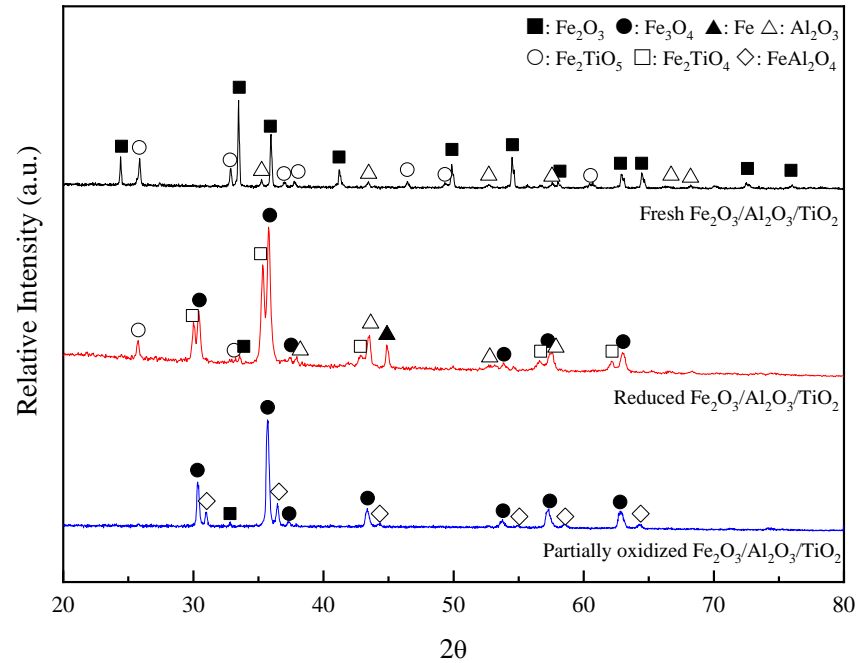
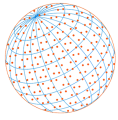


Fig. 11. X-ray diffraction patterns of fresh, reduced and partially oxidized $\text{Fe}_2\text{O}_3/\text{Al}_2\text{O}_3/\text{TiO}_2$ oxygen carriers.

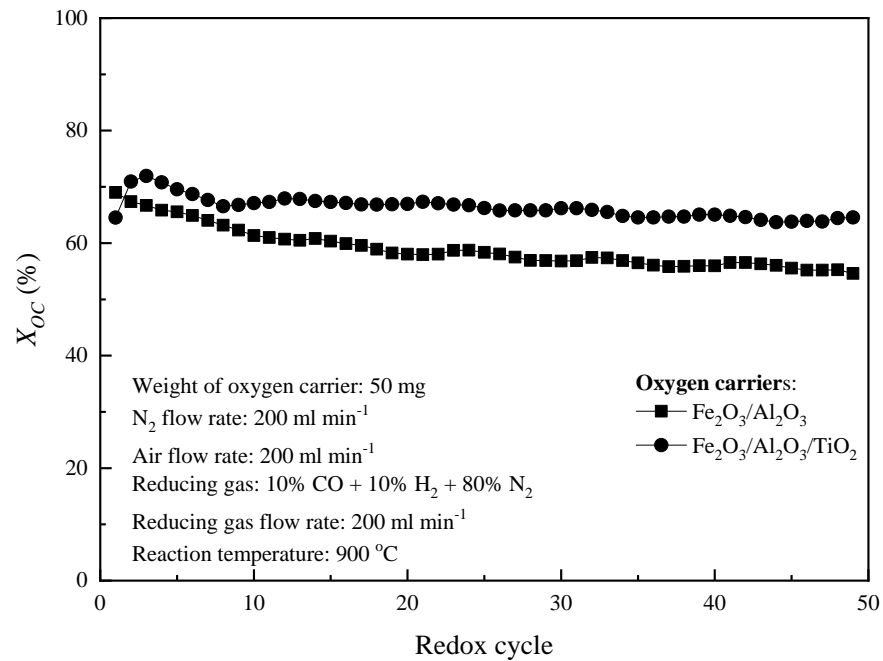
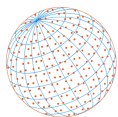


Fig. 12. Oxygen carrier conversions of regenerated oxygen carriers with syngas conducted in the TGA at 900°C .

reduced iron and aluminum species being oxidized to Fe_3O_4 and FeAl_2O_4 . This was also observed by previous researchers (Zhao and Shadman, 1990), where phase separation took place during the reduction of Fe_2O_3 and TiO_2 , with iron species moving out to the outer surface in a thermodynamically driven process.

Finally, the reactivity of regenerated oxygen carriers was examined using syngas as the reducing gas in TGA for 50 successive redox cycles. As depicted in Fig. 12, the conversions of $\text{Fe}_2\text{O}_3/\text{Al}_2\text{O}_3$ and $\text{Fe}_2\text{O}_3/\text{TiO}_2/\text{Al}_2\text{O}_3$ remained at about 55 and 65%, respectively, after 50 redox



cycles. Comparing this to Fig. 2, displaying TGA results of freshly fabricated oxygen carriers using the same parameters, shows some interesting patterns. After 50 cycles, $\text{Fe}_2\text{O}_3/\text{Al}_2\text{O}_3$ oxygen carrier conversion was shown to be 51.0% with fresh oxygen carriers and 54.6% after regeneration. For $\text{Fe}_2\text{O}_3/\text{TiO}_2/\text{Al}_2\text{O}_3$ this was 56.4 and 64.6% with fresh and regenerated oxygen carrier, respectively. This indicates that the regenerated oxygen carriers could provide reasonable reactivity and recyclability for continuous redox cycling with syngas combustion, with $\text{Fe}_2\text{O}_3/\text{TiO}_2/\text{Al}_2\text{O}_3$ oxygen carriers displaying a higher benefit from regeneration.

4 CONCLUSIONS

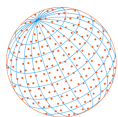
Chemical looping hydrogen generation was performed using fabricated $\text{Fe}_2\text{O}_3/\text{Al}_2\text{O}_3$ and $\text{Fe}_2\text{O}_3/\text{TiO}_2/\text{Al}_2\text{O}_3$ oxygen carriers. Initial TGA tests revealed that conversion at 900°C was very comparable between oxygen carriers, remaining between 50 and 55%. The oxygen carriers were reduced to 33% inside a fixed-bed reactor for further steam conversion experiments. For steam regeneration inside a moving-bed reactor an increase in temperature from 800 to 850°C caused no significant increase but a further increase to 900°C led to an increased steam conversion. A higher steam flow rate generally led to higher hydrogen concentrations and flow rates but lower overall steam conversions. $\text{Fe}_2\text{O}_3/\text{Al}_2\text{O}_3$ oxygen carriers displayed a higher H_2 concentration than $\text{Fe}_2\text{O}_3/\text{TiO}_2/\text{Al}_2\text{O}_3$. Steam conversion efficiency initially increased with flow rate of reduced oxygen carrier but at higher rates led to no significant improvement or even to a minor decrease in efficiency. A steam conversion of 65.2% and 78.6% was measured for $\text{Fe}_2\text{O}_3/\text{Al}_2\text{O}_3$ and $\text{Fe}_2\text{O}_3/\text{TiO}_2/\text{Al}_2\text{O}_3$ oxygen carriers, respectively. X-ray diffraction was performed on oxygen carriers that were fresh, reduced and partially oxidized in the steam reactor. A final comparison was performed with a conversion of 54.6% and 64.6% for $\text{Fe}_2\text{O}_3/\text{Al}_2\text{O}_3$ and $\text{Fe}_2\text{O}_3/\text{TiO}_2/\text{Al}_2\text{O}_3$ oxygen carriers after 49 cycles.

ACKNOWLEDGEMENTS

This research was supported by Grant MOST 104-3113-E-007-001- from the National Science and Technology Program-Energy, Taiwan.

REFERENCES

- Abad, A., Mattisson, T., Lyngfelt, A., Johansson, M. (2007). The use of iron oxide as oxygen carrier in a chemical-looping reactor. *Energy Fuels* 86, 1021–1035. <https://doi.org/10.1016/j.fuel.2006.09.021>
- Adánez, J., Cuadrat, A., Abad, A., Gayán, P., de Diego, L.F., García-Labiano, F. (2010). Ilmenite activation during consecutive redox cycles in chemical-looping combustion. *Energy Fuels* 24, 1402–1413. <https://doi.org/10.1021/ef900856d>
- Cabello, A., Abad, A., García-Labiano, F., Gayán, P., de Diego, L.F., Adánez, J. (2014). Kinetic determination of a highly reactive impregnated $\text{Fe}_2\text{O}_3/\text{Al}_2\text{O}_3$ oxygen carrier for use in gas-fueled Chemical Looping Combustion. *Chem. Eng. J.* 258, 265–280. <https://doi.org/10.1016/j.cej.2014.07.083>
- Chiu, P.C., Ku, Y., Wu, H.C. Wu, Y.L., Tseng, Y.H., Kuo, Y.L. (2014). Characterization and evaluation of prepared $\text{Fe}_2\text{O}_3/\text{Al}_2\text{O}_3$ oxygen carriers for chemical looping process. *Aerosol Air Qual. Res.* 14, 981–990. <https://doi.org/10.4209/aaqr.2013.04.0135>
- Cho, P., Mattisson, T., Lyngfelt, A. (2006). Defluidization conditions for fluidized-bed of iron, nickel, and manganese oxide containing oxygen-carriers for chemical-looping combustion. *Ind. Eng. Chem. Res.* 45, 968–977. <https://doi.org/10.1021/ie050484d>
- Cuadrat, A., Abad, A., García-Labiano, F., Gayán, P., de Diego, L.F., Adánez, J. (2011). The use of ilmenite as oxygen-carrier in a 500 Wth Chemical-Looping Coal Combustion unit. *Int. J. Greenhouse Gas Control* 5, 1630–1642. <https://doi.org/10.1016/j.ijggc.2011.09.010>
- Fan, L.S. (2010). *Chemical looping systems for fossil energy conversions*. John Wiley & Sons, Inc.
- Hurst, S. (1939). Production of hydrogen by the steam-iron method. *Oil & Soap Feb.*



- Kierzkowska, A.M., Bohn, C.D., Scott, S.A., Cleeton, J.P., Dennis, J.S., Müller, C.R. (2010). Development of iron oxide carriers for chemical looping combustion using sol-gel. *Ind. Eng. Chem. Res.* 49, 5383–5391. <https://doi.org/10.1021/ie100046f>
- Li, F.X., Luo, S.W., Sun, Z.C., Bao, X.G., Fan, L.S. (2011). Role of metal oxide support in redox reactions of iron oxide for chemical looping applications: Experiments and density functional theory calculations. *Energy Environ. Sci.* 4, 3361–3667. <https://doi.org/10.1039/c1ee01325d>
- Lo, M.C. (2011). Composite Fe-Ti based oxygen carrier for chemical looping combustion and hydrogen generation. Master Thesis in Department of Chemical Engineering, National Taiwan University of Science and Technology, Taipei City, Taiwan.
- Mattisson, T., Johansson, M., Lyngfelt, A. (2004). Multicycle reduction and oxidation of different types of iron oxide particles - Application to chemical-looping combustion. *Energy Fuels* 18, 628–637. <https://doi.org/10.1021/ef0301405>
- Sun, S.Z., Zhao, M., Cai, L., Zhang, S., Zeng, D.W., Xiao, R. (2015). Performance of CeO₂-modified iron-based oxygen carrier in the chemical looping hydrogen generation process. *Energy Fuels* 29, 7612–7621. <https://doi.org/10.1021/acs.energyfuels.5b01444>
- Tong, A., Sridhar, D., Sun, Z., Kim, H.R., Zeng, L., Wang, F., Wang, D., Kathe, M.V., Luo, S., Sun, Y., Fan, L.S. (2013). Continuous high purity hydrogen generation from a syngas chemical looping 25 kW_{th} sub-pilot unit with 100% carbon capture. *Fuel* 103, 495–505. <https://doi.org/10.1016/j.fuel.2012.06.088>
- Yang, J.B., Cai, N.S., Li, Z.S. (2008). Hydrogen Production from the steam-iron process with direct reduction of iron oxide by chemical looping combustion of coal char. *Energy Fuels* 22, 2570–2579. <https://doi.org/10.1021/ef800014r>
- Zhao, Y., Shadman, F. (1990). Kinetics and mechanism of ilmenite reduction with carbon monoxide. *AIChE J.* 36, 1433–1438. <https://doi.org/10.1002/aic.690360917>
- Zieliński, J., Zglinicka, I., Znak, L., Kaszukur, Z. (2010). Reduction of Fe₂O₃ with hydrogen. *Appl. Catal., A* 381, 191–196. <https://doi.org/10.1016/j.apcata.2010.04.003>